

Drilling Performance of Aluminum Plates under Manual Drilling Conditions

Yasuo Kondo* and Youji Miyake

Department of Mechanical System Engineering, Yamagata University, Yonezawa, Japan
Email: kondo@yz.yamagata-u.ac.jp (Y.K.); youjiyasuo@ymail.ne.jp (Y.M.)

*Corresponding author

Abstract—There are more than 1.3 million holes in a typical large aircraft. The drilling is made by a variety of processes. For components that cannot be mounted on a CNC machine, drilling is made on-site after the components are assembled together. Many efforts have led to the increasing use of robots and special tools for on-site drilling, but manual drilling is still often used. In this study, a simple drilling model was designed that can make holes in a similar procedure to manual drilling, without human assistance. The experiments focused on the drilling under conditions where the workpiece deflects during machining. In the proposed drilling method, the load $P(N)$ applied to the cutting edge is the critical operating parameter for burr formation. The simple model had a suitable P that can suppress burr formation. To develop an automated tool based on the proposed method, it is necessary to identify the optimum control conditions for applied load P .

Keywords—drilling, burr formation, manual operation, thrust force, deflection

I. INTRODUCTION

Aluminum alloy is widely used in aircraft structure components due to its superior strength-to-weight ratio. According to some reports, there are more than 1.3 million holes in a typical large commercial aircraft [1, 2]. An aircraft fuselage or wing consists of multiple large-scale skin sheets mounted on supporting structure such as stringers and frames. These unusual structures of aircraft require specific assembly and drilling methods. A distinctive assembly method called One Way Assembly (OWA) has been applied to the assembly of aircraft where many holes are machined after the components are assembled together [3].

In the assembly of automobiles and other products, the assembly work is typically processed in the following order: 1. Processing the shape for each component. 2. Drilling holes on each component. 3. Assembling the components together. In this case, most holes can be machined using Numerical Control (NC) machine tools. In the OWA cell, the drilling is made by a variety of processes. As with many products, drilling is made on the NC machine tools for components that can be attached to the NC machine tools. For components that cannot be

mounted on NC machine tools, drilling is performed on-site after the components are assembled together. In this situation, the drilling is accomplished in one of the following three ways: by robot, by specialized machine, or manually [4–8].

The use of robotic drilling has become popular in aircraft assembly due to its accessibility, lower investment costs and increasing level of automation [9]. Since the beginning of the 21st century, studies on robotic drilling have been carried out in the USA, Germany, Italy and other countries [10]. In many cases, the robotic drilling system is designed to automate the drilling required in aircraft assembly. The system is typically set up as a frame structure, drilling unit, pressing unit, measuring unit, robot flange and electrical control unit [11]. This means that the drilling system will be large and heavy. Considering the low rigidity of the robot arm, the heavy weight of the system is not advantageous for the robotic drilling. Therefore, the application of robotic drilling to on-site drilling is limited [12, 13].

Some special drilling methods have been developed to overcome the low stiffness of the industrial robot arm [12, 13]. Non-contact drilling methods such as laser machining, electric discharge machining and electrochemical machining are recommended for use in this application [13]. These machining methods have low values of material removal rates, but they can also damage the properties of work material due to high heat affected zone and intergranular corrosion attack. A rotary ultrasonic drilling machine was also developed [14–17]. This machine is mounted on industrial robot arms to reduce the cutting force and vibration. Ultrasonic drilling is said to be a potential solution for low-stiffness robotic drilling. However, it requires some expensive equipment other than the spindle and has limited applicability.

These efforts have led to the increasing use of robots and special tools for on-site drilling. However, manual drilling is still often used. From the relevant literature and websites, the manual drilling is often applied in the following situations; the materials to be machined have a beam or shell structure, so the materials will deflect during the drilling, two or more plates are simultaneously machined, and many of the materials to be machined will have curved surfaces [3, 18–19]. Particularly, drilling under conditions where the workpiece deflects during

Manuscript received May 16, 2023; revised July 13, 2023; accepted July 25, 2023; published January 24, 2024.

machining is said to be difficult with existing automated tools [18, 19].

The authors have been developing a drilling method that can make holes with no burr formation under the conditions that cannot be automated with currently available tools [20, 21]. Unlike conventional automated tools, the developing drilling method directly replicates manual drilling. There are no work standards for manual drilling, but the operator performs a series of steps: picks up the electric drill, applies load to the drill, drills the hole, and then puts the drill down [22]. Even in the operation with manual drilling machines, the operator performs the similar operation. This suggests that the hole can be drilled by controlling the force to push the electric drill or spindle in the manual drilling, while most automated drilling tools have a mechanism to precisely control the tool feed rate like NC machine tools. The developing drilling method can make holes by controlling the force to push the spindle as in the case of manual drilling. The drilling with the developing drilling method will be called “soft-machining”.

In this study, a simple drilling model using soft machining was designed. The simple model can make holes in a similar way to manual drilling, without human assistance. Using the simple model, holes were drilled in aluminum plates under conditions where the workpiece is easily deflected during machining. The relationship between cutting conditions and burr formation was examined, and the operating conditions to suppress burr formation were also discussed.

II. EXPERIMENTAL

A. Target Drilling Condition

According to the relevant literature and websites [1–3, 18–19], manual drilling is still often applied in the following situations:

- 1) The materials to be machined have a beam or shell structure, so the materials will deflect during drilling.
- 2) Two or more plates are machined simultaneously.
- 3) Many of the materials to be machined have curved surfaces.
- 4) The plates to be machined simultaneously may not be of the same material.

Fig. 1 shows examples of on-site manual drilling work [3]. These conditions definitely make drilling more challenging. In particular, the deflection of the workpiece during drilling is a troublesome problem because it accelerates burr formation. In addition, the formation of interlayer burr becomes an additional problem in the simultaneous drilling of stacked plates. Once burrs form, deburring work is required [1, 2].

Unfortunately, no recognized standard testing method exists to examine the effect of the deflection of the workpiece on burr formation. In this study, based on the relevant literature [1–2, 18–19], four clamping conditions for the workpiece are set as shown in Table I. The number of plates to be drilled at one time was one or two. In the case of a single plate, entrance and exit burrs are critical concerns. In the case of stacked plates, the

interlayer burr becomes a critical concern. For both single and stacked plates, there are two possible cases: one is the case where the workpiece deflects during drilling and the other is the case where it does not.



Fig. 1. Drilling in aircraft assembly.

TABLE I. VARIETY OF CLAMPING CONDITIONS OF WORKPIECES

Clamping device	Vice (No deflection)		Bolts and nuts (Allow deflection)	
	Yes	No	Yes	No
Simultaneous drilling of stacks with two plates	Yes	No	Yes	No

B. Modeling of Manual Drilling

Fig. 2 summarizes the development process of the simple model used in this study. The developed model directly reproduces manual drilling, where the hole is drilled by controlling the force to push the electric drill or spindle. It has been reported that operators push the electric drill with a force of around 40 N in manual operations [22]. In the original design shown in Fig. 2(a), the tool is fed by a weight placed on top of the spindle. To control the feed direction, the spindle is connected to the linear guide. In this model, a weight of about 4 kg has to be placed on the spindle to load 40 N, which is not very practical. Fig. 2(b) shows the upgraded model. The upgraded model has the feed mechanism commonly used in conventional drill stands, which reduces the mass of the weight required to feed the tool. In the drilling with this type of tool, the operator applies force to the end of the tool feed handle. In the upgraded model, the force required to feed the tool is provided by a weight of $W(g)$ suspending on the tool feed handle, as shown in Fig. 2(c). By using weights, holes can be drilled without human assistance. In this study, the upgraded model is termed the “simple model”.

Before conducting the experiments with the simple models, the operating parameters of the drilling tool need to be clarified. The mass $W(g)$ of the weight cannot be used as an operating parameter because it varies depending on the tool feed mechanism. In this study, the load $P(N)$, the load acting on the tool cutting edge, was introduced as an operating parameter of the simple model. $P(N)$ is an original parameter of this study and is considered to be close to the thrust force.

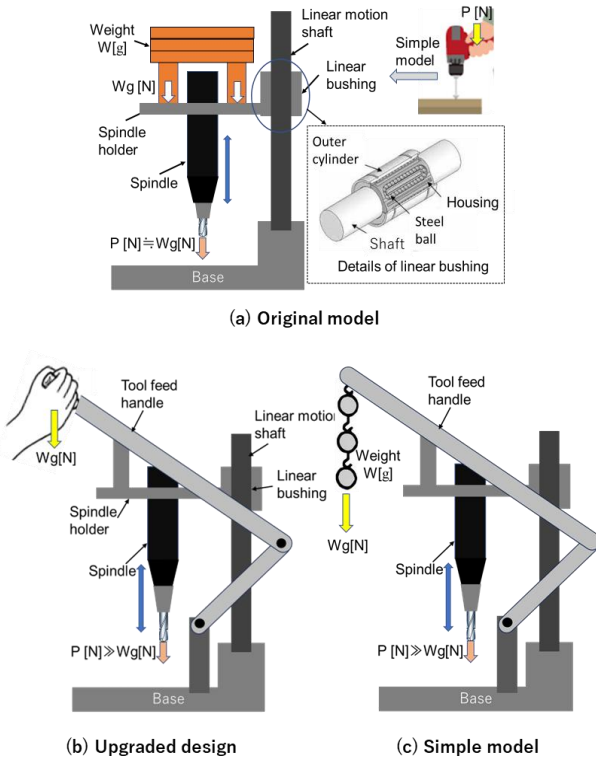


Fig. 2. (a) Original model, (b) Upgraded design and (c) Simple model Development process of simple model.

$P(N)$ correlates with $W(g)$ once the type of drilling tool, workpiece material, tool geometry and cutting conditions were determined. Fig. 3 shows the relationship between the mass $W(g)$ of the weight and the load $P(N)$ acting on the tool cutting edge, in the drilling with the simple model. This relationship is based on the measured values obtained by drilling the “workpiece integrated with the load cell” using the simple model. The details of the “workpiece integrated with the load cell” are shown in Fig. 4. A brass workpiece attachment is fixed to a digital force gauge (CNYST Co., Ltd. YST-300), and the workpiece to be drilled is fixed to the workpiece attachment with double-sided adhesive tape. Drilling was then conducted by holding the “workpiece integrated with the load cell” in a vice. In the range examined, $P(N)$ and $W(g)$ showed a proportional relationship. This means that the load $P(N)$ acting on the cutting edge can be controlled by the mass $W(g)$ of the weight.

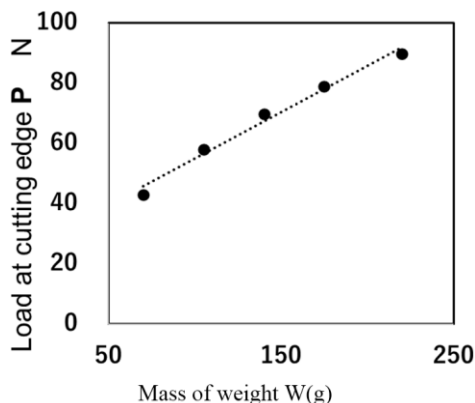


Fig. 3. Relationship between mass of the weight W and the load P .

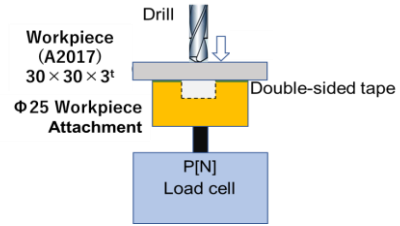


Fig. 4. Details of “workpiece integrated with the load cell”.

Fig. 5 shows the change in $P(N)$ during the drilling with P of around 80 N. In this cutting condition, the average tool feed rate was about 48.6 mm/min. Fig. 5 also shows the change in $P(N)$ when drilling holes at a tool feed rate of 48.6 mm/min using a conventional NC machine. The appearance of the hole entrance and exit is also shown. The used NC machine and the drilling tool used for soft machining are equipped with the same type of spindle. The soft machining keeps the P at around 80 N during drilling, whereas the P reaches around 140 N in drilling with NC machine. Moreover, the soft machining suppresses visible burr formation, whereas NC machines forms a crown-shaped burr.

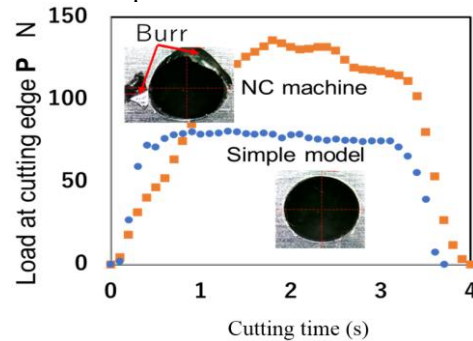


Fig. 5. Change in P during drilling with P of around 80 N.

Most automated drilling tools have a mechanism to precisely control the tool feed rate, like NC machines. Burr formation is a complex mechanical process. In general, burr formation is strongly related to the thrust force. Excessive thrust force results in the formation of a tall ring or crown-shaped burr, as shown in Fig. 6 [23]. The thrust force is said to be determined by the tool geometry, hole diameter, workpiece material, cutting condition, etc. In drilling of aluminum plates by usual NC machines, the tool feed rate is the most significant parameter influencing the burr height, followed by the drill diameter, point angle, etc., while the influences of cutting speed could be neglected [24]. In most cases, the thrust force is controlled by the tool feed rate and many reports show that the thrust force in the drilling of aluminum plates is in the range of 100–1000 N [1–2, 18–19, 23–24]. The relationship in Fig. 3 shows that the simple model can make holes with a thrust force of less than 100 N. The smaller thrust force in the simple model is expected to suppress burr formation.

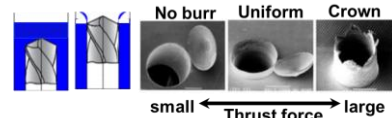


Fig. 6. Type of exit burr in drilling with standard twist drill.

C. Cutting Conditions

The present study focuses on the fact that the components to be drilled have a shell or beam structure because it is well known that the deflection of the component often enhances the formation of burrs and other defects in the drilling process. The cutting conditions are shown in Table II. A short drill made of cobalt HSS with a diameter of 4 mm and a tip angle of 135° was used. The workpiece materials used were A2017 and A7075 aluminum alloy. These alloys are widely used as aircraft materials. The configuration and clamping conditions of the workpiece were determined based on the previous studies that studied the effect of deflection of workpiece on burr formation [18–19, 23–26]. To examine the effect of deflection on burr formation, the workpiece was clamped in a vice or bolted at both ends, as shown in Fig. 7. No deflection occurs when clamped in a vise, while deflection occurs when fixed with bolts and nuts. The dimensions of the workpiece were 3mm thick, 25mm wide, and 100mm long for clamping by a vice, and 3 mm thick, 25 mm wide, and 150 mm long for clamping by bolts and nuts. The number of plates to be drilled at one time was one or two. In the drilling of stacked plates, the two plates were fixed in close contact and two plates were processed simultaneously at once under the same cutting conditions.

TABLE II. CUTTING CONDITIONS

Cutting tool	Cobalt HSS $\Phi 4\text{mm}$ 135° of point angle			
Spindle speed [rpm]	2000			
Material	Plate		Stack (upper / lower)	
	A2017	A7075	A2017/A2017 A7075/A7075	A2017/A7075 A7075/A2017
Young's modulus [MPa]	69000	71000	69000 / 69000 71000 / 71000	69000 / 71000 71000 /69000
Applied load [N]	35	60	60 85 110	
Dimension [mm]	$25^w \times 100^l \times 3^t$ or $25^w \times 150^l \times 3^t$			

Five or six holes were drilled continuously at intervals of 10 mm in the longitudinal direction. The hole locations are also shown in Fig. 7. The workpiece was basically set horizontally on the table surface and bolted to the table with an appropriate torque. The cutting speed was 2000 rpm and the applied load P was varied in the range of 35–110 N. In the soft machining, P is a critical operating parameter. If P is too small, the hole cannot be drilled and the drill tip continues idling on the workpiece surface. To determine the optimum value of P , the P values were varied from the minimum P required to make a hole. After drilling under each cutting condition, observation of hole shape and burr formation was done by using a microscope. Burr height and scratch depth were determined by measuring the cross-sectional profile with a stylus surface profiler capable of nm-scale measurement (BRUKER DECTAC-XTL). The DECTACK is able to determine the cross-sectional shape without cutting the sample. This study focused on examining the formation

of burrs, so detailed measurements of the burr and hole configuration were not conducted.

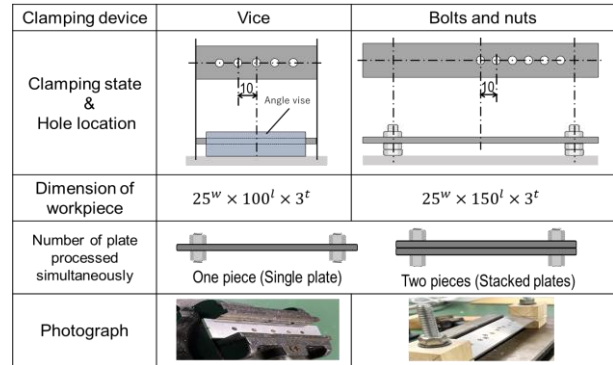


Fig. 7. Clamping conditions of workpiece.

III. RESULT AND DISCUSSION

A. Burr Formation in Drilling of Single Plate

In this study, a total of more than 200 holes were drilled. All drilling was conducted with just one drill, but there was no reduction in cutting speed. Fig. 8 shows the appearance of workpiece after drilling holes in A2017 and A7075. In this case, the workpiece was clamped with bolts and nuts to allow the deflection of workpiece during drilling. The loads P were 35 N for A2017 and 60 N for A7075, which were the minimum loads that could drill the hole. At loads below the minimum load, the drill did not be able to make a hole.

The soft machining did not form visible burrs under almost all conditions. Fig. 8 includes a magnified view of the exit side for some holes. It is difficult to recognize burrs without microscopic observation because they have very low height and appear only on limited areas of the hole. Only small burrs tended to form in the holes near the fixed end, while no noticeable defects were found in the holes far from the fixed end, regardless of the material. Fig. 9 shows the appearance of the entrance and exit of the hole after drilling A2017 under conditions where no deflection of the workpiece occurs during drilling. Under such conditions, no burr formation was observed regardless of the hole location.

In general, the deflection of workpiece during drilling strongly affects burr formation [18–19, 23–26]. Teimouri *et al.* showed that in the drilling of aluminium plates using conventional drilling methods, about 400–1000 N thrust forces act and 78–189 microns of deflection are generated. In this condition, it is often recognized that a crown-shaped exit burr is formed [26]. Fig. 10 shows the deflection curve of a beam with a span of 150 mm when a concentrated load of 40 N is applied to the beam at $a=25, 35, 45, 44, 65,$ and 75 mm. The location of load points corresponds to the center of the drilled holes in Fig. 8. The small burrs were found in the holes at positions $a=25$ and 35 . In these two positions, the deflection, around $5 \mu\text{m}$, is smaller than in the other positions, around $15 \mu\text{m}$. These facts indicate that lower thrust forces in soft machining do not lead to enough deflection to affect burr

formation. Namely, drilling with lower thrust forces, such as soft machining, can significantly suppresses burr formation even under challenging conditions where the workpiece is easily deflected during machining.

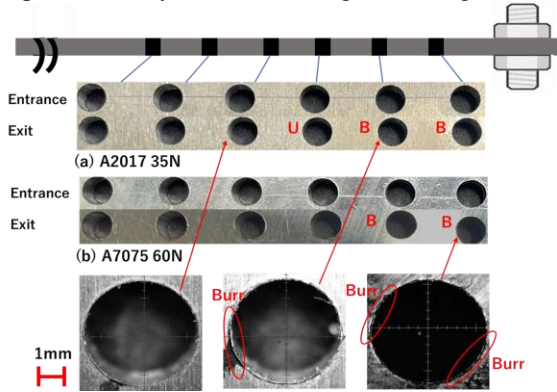


Fig. 8. Appearance of workpiece after drilling in A2017 and A7075.

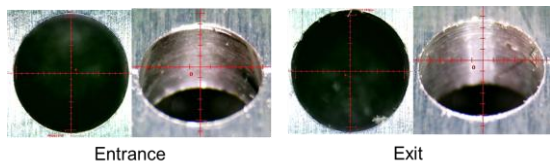


Fig. 9. Appearance of hole after drilling A2017 with no deflection.

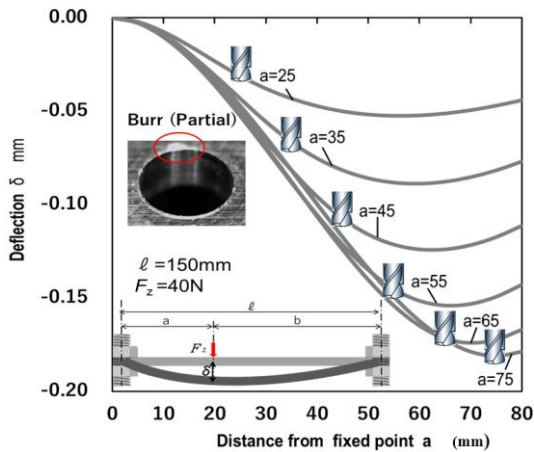


Fig. 10. Deflection of workpiece when a concentrated load is applied.

B. Burr Formation in Drilling of Stacked Plates

Fig. 11 shows burr formation when A2017/2017 stack plates are drilled under conditions where no deflection of

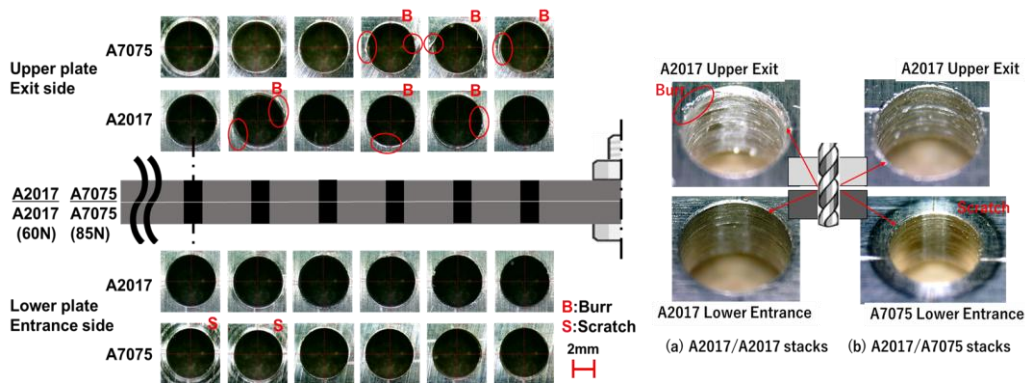


Fig. 11. Burr formation in drilling A2017/A2017 with no deflection.

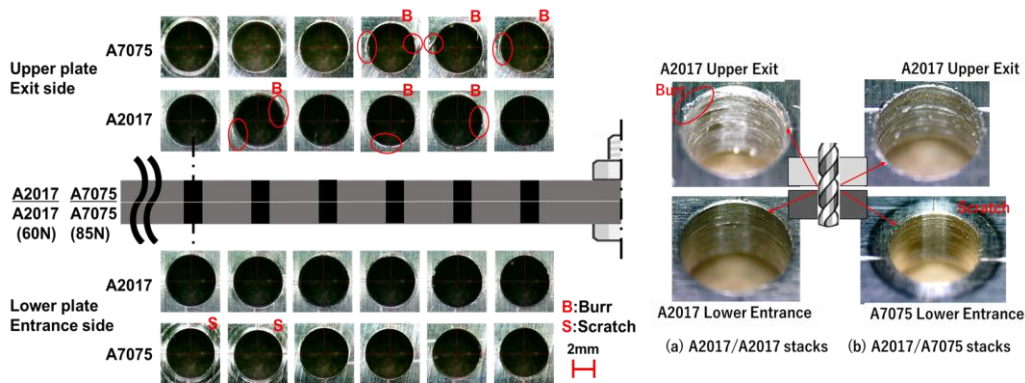


Fig. 12. Appearance of workpiece after drilling in stacked plates from the same material.

the workpiece occurs. The minimum load P required for drilling was 60 N for A2017 and 85 N for A7075. As in the case of the single plate, no visible entrance, exit and interlayer burrs were observed in all machined holes. Fig. 12 shows the appearance of the machined hole when the through holes were machined on A2017/A2017 or A7075/A7075 stacked plate with a load P of 85N under conditions where the workpiece is easily deflected during drilling. In Fig. 12, only the appearance of the exit side of the upper plate and the entrance side of the lower plate are shown because interlayer burrs that form between the upper and lower plates are often problem in the drilling of stacked plates [23, 25]. Even in the drilling of stacked plates, the soft-machining was able to make through holes at the specified points in all cutting conditions and no noticeable burrs were observed at the entrance of the upper plate and at the exit of the lower plate from the observation by a digital microscope. However, damages were found on the contact surfaces of the two plates; an exit burr on the upper plate and a circumferential scratch at the contact surface of lower plate. A small interlayer burr tended to form in the holes near the fixed end, while no noticeable defects were found in the holes far from the fixed end, as was the case with the single plate. In addition, a circumferential scratch was found on the contact surface of lower plate when A7075/A7075 stacked plates was drilled.

Fig. 13 shows the appearance of the workpiece when the through holes were machined on A2017/A7075 or A7075/A2017 stacked plate with a load P of 85N. Even in the drilling of stacked plates made up from different materials, the soft machining was able to machine through holes under all cutting conditions. No noticeable defects were observed at the entrance of the upper plate

and at the exit of the lower plate. Only small interlayer burrs and circumferential scratches tended to form under the same conditions as in the case of stacked plates made up from the same material. In contrast, no reports have been found that scratches had appeared in the conventional drilling.

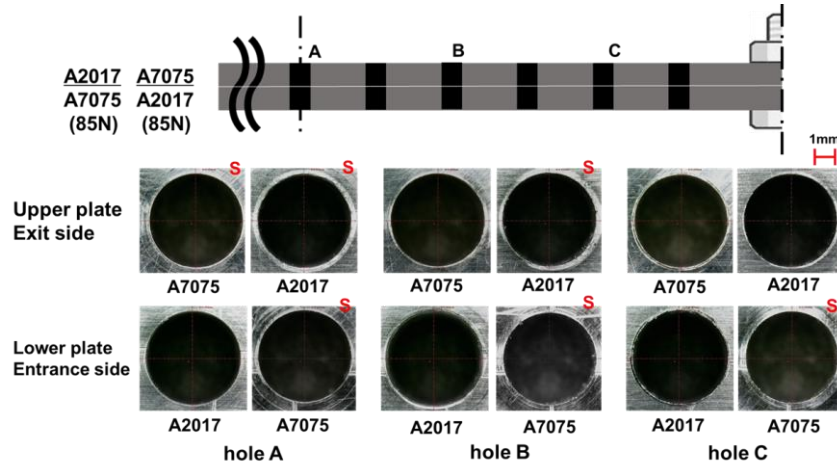


Fig. 13. Appearance of workpiece after drilling in stacked plates from different materials.

Fig. 14 shows typical chip shapes formed during drilling of A2017 and A7075. A2017 tends to generate a long spiral chip while A7075 tends to generate short shredded chips. Short shredded chips may easily get into the gap between the contact surfaces and cause damage around the hole; the circumferential scratches are related to the shape of the chips generated from the lower plate. This is considered to be related to the fact that the soft machining has much lower tool feed rate than that in the conventional drilling as shown in Table III. The smaller feed rates result in thinner chip, so the chips are more likely to break and become chipped.

Fig. 15 shows the appearance and cross-sectional profiles of an interlayer burr and a scratch. These were determined by measuring the surface profile with a stylus surface profiler DECTAC-XTL that is able to determine cross-sectional surface profiles non-destructively. Burrs formed on a part of the hole circumference and their height was about 100 μm. The depth of the circumferential scratch was less than 100 nm and is considered not to affect the assembly accuracy and strength of the component. In this way, the soft machining can significantly suppress the formation of stacked burrs and other defects even in the drilling of stacked plates under cutting conditions where the workpiece is easily deflected during machining. However, A small interlayer burrs tended to form in the holes near the fixed end.

TABLE III. FEED RATE OF DRILL THROUGH UPPER AND LOWER PLATES

Reference	Type	Material	Feed rate [mm/r]
Present work	Plate	A2017	0.0028 ~ 0.0042
		A7075	0.0006 ~ 0.001
	Stack	Upper A2017	0.0015 ~ 0.002
		Lower A7075	0.0003 ~ 0.0005
	Stack	Upper A7075	0.0017 ~ 0.0024
		Lower A2017	0.0006 ~ 0.005
Nouari [27]	Plate	A2024	0.04
Rivero [28]	Plate	A7075	0.3
Bu [25]	Plate	A7475	0.05 ~ 0.3
Lei [29]	Stack	Upper A2024	0.033
		Lower A2024	
Dong [30]	Stack	Upper CFRP	0.012 ~ 0.024
		Lower A7075	

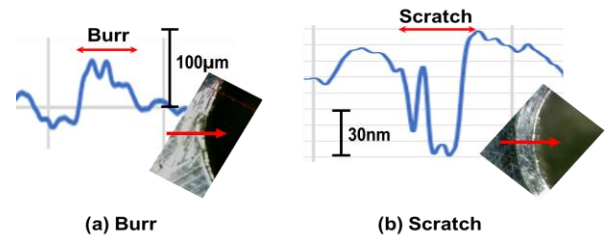


Fig. 15. Appearance and cross-sectional profiles of burr and scratch.

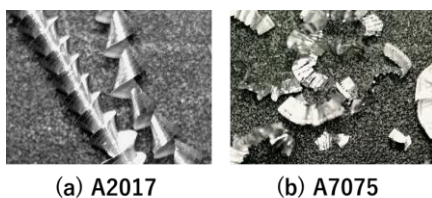


Fig. 14. Typical chip shapes formed in drilling of A2017 and A7075.

C. Effect of Applied Load on Hole Quality

Fig. 16 shows the deflection of the workpiece during drilling of A2017/A2017 stacked plates with loads P of 60 N, 85 N and 110 N. These photographs were taken when the drill penetrated the upper plate. The deflection of the workpiece strongly depends on the load P. At a load p of 60 N, no visible interlayer gap was found and there is no significant change in the state of deflection during the drilling. With a load P of 85 N or more, a gap

is created between the upper and lower plates when the drill penetrates the upper plate. Once the cutting of the lower plate began, the gap became smaller at a load P of

85N while, no change in clearance size was observed at a load P of 110 N.

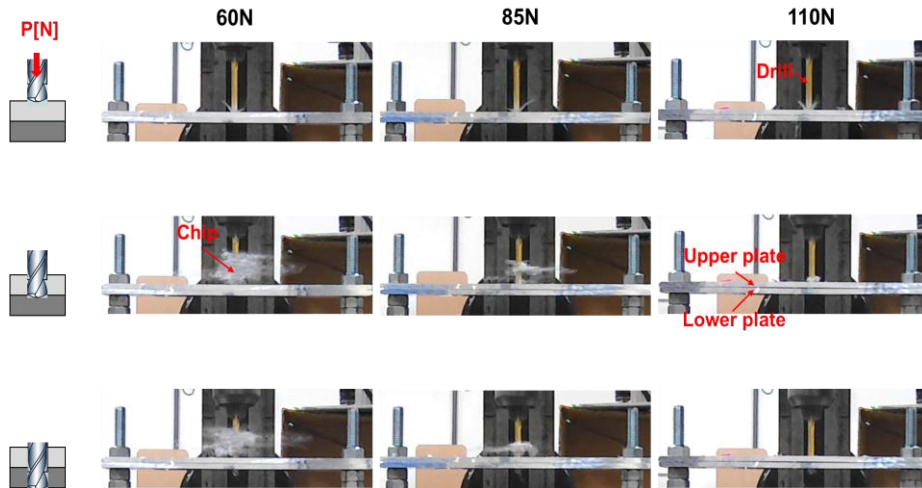


Fig. 16. Deflection of workpiece during drilling of A2017/A2017 stacked plates.

Fig. 17 shows the appearance of the holes obtained from the drilling with loads P of 60, 85 and 110 N. The photo shows the appearance of the holes at locations A, B, and C on the exit side of the upper plate and on the entrance side of the lower plate. The formation of interlayer burrs becomes more pronounced as the load increases. In the machining with a load P of 110 N, the interlayer gap is continuously formed, and the formation of burrs is also noticeable as shown in Fig. 18.

make cutting and tool feeding. With a load greater than 60 N, the excessive load leads to deformation of the workpiece, which then promotes the formation of burrs and other defects.

IV. CONCLUSION

To reduce labor in aircraft assembly, a drilling tool was designed that directly reproduces manual drilling. The basic performance of the tool was experimentally examined, focusing on drilling under conditions where the workpiece deflects during machining. In the proposed drilling method, the load $P(N)$ applied to the cutting edge is the critical operating parameter for burr formation. A simple model was able to suppress burr formation even under conditions where the workpiece deflects during drilling, but there are still many unknowns. To develop an automated tool based on the proposed drilling method, it is necessary to quantitatively evaluate the relationship between load P and burr formation and to identify the optimum control conditions for P . In addition, detailed measurement of the burr and hole configuration must also be conducted in order to use soft machining as a practical automated tool.

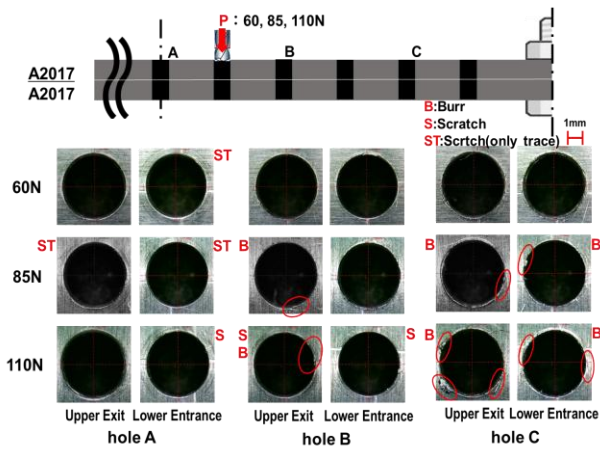


Fig. 17. Damages from the drilling with loads of 60, 85 and 110 N.

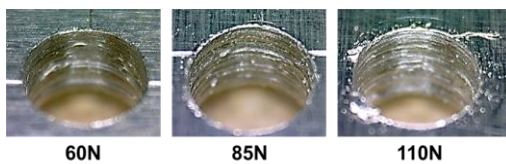


Fig. 18. Effect of applied load P on burr formation.

These facts indicate that the formations of burrs and other defects can be suppressed by optimizing the applied load P in the soft-machining. From the results of this study, it is considered that a load P of around 60 N is optimum and this is about the minimum load that can

CONFLICT OF INTEREST

The authors declare no conflict of interest.

AUTHOR CONTRIBUTIONS

Yasuo Kondo conducted the research and wrote the paper; Youji Miyake analyzed the data. Both authors had approved the final version.

FUNDING

This work was partly supported by The MIKIYA Science and Technology Foundation.

REFERENCES

- [1] Y. Bu, W. H. Liao, W. Tian, J. X. Shen, and J. Hu, "An analytical model for exit burrs in drilling of aluminum materials," *Int J Adv Manuf Technol*, vol. 85, pp. 2783–2796, 2016.
- [2] J. Choi, S. Min, D. A. Dornfeld, M. Alam, and T. Tzong, "Modeling of inter-layer gap formation in drilling of multi-layered material," in *Proc. 6th CIRP Workshop on Modeling of Machining*, McMaster University, Hamilton, pp. 36–41, 2003.
- [3] Robodk. [Online]. Available: <https://robodk.com/blog/end-effector-for-robot-drilling/>.
- [4] R. Devlieg, K. Sittou, E. Feikert, and I. Inman, "ONCE(ONe-sided Cell End-effector), robotic drilling system," in *Proc. SAE2002 Automated Fastening Conference and Exposition*, Chester, ENGLA.SAE Technical Papers 2002–01–2626, 2002.
- [5] J. Atkinson, J. Hartmann, S. Jones, and P. Gleeson, "Robotic drilling system for 737 aileron," in *Proc. SAE2007 Aero Tech Congress and Exhibition*, Los Angeles, CA, USA. SAE Technical Papers 2007–01–3821, 2007.
- [6] W. Zhu, W. Qu, L. Cao, D. Yang, and Y. Ke, "An off-line programming system for drilling in aero-space manufacturing," *Int. J. Adv. Manuf. Technol.*, vol. 68, pp. 2535–2545, 2013.
- [7] Y. Guo, H. Dong, and Y. Ke, "Stiffness-oriented posture optimization in robotic machining applications," *Robot. Comput. Integr. Manuf.*, vol. 35, pp. 69–76, 2015.
- [8] V. Krishnaraj, R. Zitoune, and F. Collombet, "Comprehensive review on drilling of multi-material stacks," *J of Mechanical and Forming Technology*, vol. 2, pp. 1–32, 2010.
- [9] L. K. Lauderbaugh, "Analysis of the effects of process parameters on exit burrs in drilling using a combined simulation and experimental approach," *J Mater Process Technol*, vol. 209, no. 4, pp. 1909–1919, 2009.
- [10] M. Summers, "Robot capability test and development of industrial robot positioning system for the aerospace industry," In: *SAE 2005 AeroTech Congress & Exhibition*, Grapevine, TX, SAE Technical Papers, 2005–01–3336, 2005.
- [11] Z. Wang, X. Qin, J. Bai, X. Tan, and J. Li, "Design and implementation of multifunctional automatic drilling end effector", *Materials Science and Engineering*, vol. 187, 012032, doi:10.1088/1757-899X/187/1/012032.
- [12] V Krishnaraj, R. Zitoune, and F. Collombet, "Comprehensive review on drilling of multimaterial stacks," *Int J of Machining and Forming Technologies*, vol. 2, no. 3/4, pp. 1–32, 2010.
- [13] E. I. Hofy, "Fundamentals of machining processes: Conventional and nonconventional processes," Boca Raton, FL, CRC press, 2013.
- [14] L. Shaomina, Z. Deyuana, L. Chunjiana, and T. Huia, "Exit burr height mechanistic modeling and experimental validation for low frequency vibration-assisted drilling of aluminum 7075-T6 alloy," *Journal of Manufacturing Processes*, vol. 56, pp. 350–361, 2020.
- [15] R. Teimouri and S. Amini, "Analytical and experimental approaches to study elastic deflection of thin strip in ultrasonic-assisted drilling process," in *Proc. ImechE, Part E: J Process Mechanical Engineering*, vol. 0, no. 0, pp. 1–14, 2017.
- [16] R. B. Pereria, "A review of helical milling process," *International Journal of Machine Tools and Manufacture*, vol. 120, pp. 27–48, 2017.
- [17] R. Voss, "Comparison of conventional drilling and orbital drilling in machining carbon fiber reinforced plastics (CFRP)," *CIRP Annals.*, vol. 65, no. 1, pp. 137–140, 2016.
- [18] R. Teimouri and S. Amini, "Analytical and experimental approaches to study elastic deflection of thin strip in ultrasonic-assisted drilling process," in *Proc. IMechE Part E: J Process Mechanical Engineering*, vol. 0, no. 0, 2017, pp. 1–14.
- [19] C. J. Min, S. Dornfeld, M. Alam, and T. Tzong, "Modeling of inter-layer gap formation in drilling of multi-layered material," in *Proc. 6th CIRP Workshop on Modeling of Machining*, McMaster University, Hamilton, 2003, pp. 36–41.
- [20] Y. Miyake and Y. Kondo, "A study on new machining method applied to a collaborative robot for drilling," *Robotic and Computer Integrated Manufacturing*, vol. 78, 102400, 2022.
- [21] Y. Miyaje and Y. Kondo, "Burr formation in drilling of aluminum plates under cutting conditions for manual operation," *J. of Physics: Conf. Ser.*, 2512, 012001, 2023.
- [22] P. Maurice, V. Padois, Y. Measson, and P. Bidaud, "Human-oriented design of collaborative robots," *Int J of Industrial Ergonomics*, vol. 57, pp. 88–201, 2017.
- [23] I. J. Stein and D. A. Dornfeld, "Influence of workpiece exit angle on burr formation in drilling intersecting holes," *Trans. North American Manufacturing Research Institute. SME*, vol. 24, pp. 39–43, 1996.
- [24] L. K. Lauderbaugh, "Analysis of the effects of process parameters on exit burrs in drilling using a combined simulation and experimental approach," *J Mater Process Technol.*, vol. 209, pp. 1909–1919, 2009.
- [25] Y. Bu, W. H. Liao, W. Tian, X. J. Shen, and J. Hu, "An analytical model for exit burrs in drilling of aluminum materials," *Int. J. Manif. Technol.*, vol. 85, pp. 2763–2769, 2016.
- [26] R. Teimouri and S. Amini, "Analytical and experimental approaches to study elastic deflection of thin strip in ultrasonic-assisted drilling process," in *Proc. IMechE Part E, J Process Mechanical Engineering*, vol. 0, no. 0, pp. 1–14, 2017.
- [27] M. Nouari, G. List, F. Girot, and G. Gehin, "Effect of machining parameters and coating on wear mechanism in dry drilling of aluminium alloys," *Int J. of Machine Tools & Manufacturing*, vol. 45, pp. 1436–1442, 2005.
- [28] A. Rivero, G. Aramendi, S. Herranz, and L. N. Lopea, "An experimental investigation of the effect of coatings and cutting parameters on the dry drilling performance of aluminium alloy," *Int. J. of Adv. Manuf. Technol.*, vol. 28, pp. 1–22, 2006.
- [29] C. Lei, C. Li, Y. Bi, and J. Li, "The optimal clamping force option for robotic drilling of stacked aluminum sheets based on shell theory," *Advanced in Mechanical Engineering*, vol. 9, pp. 1–9, 2017.
- [30] S. Dong, W. Liao, K. Zheng, J. Liu, and J. Feng, "Investigation on exit burr in robotic rotary ultrasonic drilling of CFRP/aluminum stacks," *Int J. of Mechanical Science*, vol. 151, pp. 868–878, 2019.

Copyright © 2024 by the authors. This is an open access article distributed under the Creative Commons Attribution License (CC BY-NC-ND 4.0), which permits use, distribution and reproduction in any medium, provided that the article is properly cited, the use is non-commercial and no modifications or adaptations are made.